JOURNAL OF GUIDANCE, CONTROL, AND DYNAMICS
Vol. 19, No. 3, May–June 1996

Characterization of Periodic Motions in Aircraft Lateral Dynamics

N. Ananthkrishnan* and K. Sudhakar†
Indian Institute of Technology, Bombay 400076, India

Limit cycles in aircraft lateral dynamics are called wing rock. Wing rock prevention and/or control is an important objective for aircraft that need to fly and maneuver at moderate to high angles of attack. This requires a characterization of wing rock periodic motions, which is our aim. Normal and large-amplitude types of wing rock are distinguished. Onset of normal wing rock occurs at a Hopf bifurcation followed by limit cycle oscillations of gradually growing amplitude. Onset of large-amplitude wing rock is similar, but the limit cycles following the Hopf bifurcation show a jump to a large-amplitude oscillation at a periodic saddle-node bifurcation. Large-amplitude wing rock is shown to be the result of lateral–longitudinal coupling in conjunction with a resonance condition. A continuation algorithm is used to track periodic solutions with varying parameters and to locate bifurcation points. A strategy to avoid large-amplitude wing rock is indicated on the basis of the study.

Nomenclature

b	= wing span
F	= Jacobian matrix of f
f	= function of state variables
g	= vector of nonlinear terms
i_x, i_z, i_{xz}	= moments of inertia
l, m, n	= roll, pitch, and yaw moment coefficients, respectively
m	= mass
p, r	= roll and yaw rates, respectively
S	= reference area
T	= time period (of periodic motion)
t	= time
V	= velocity
x	= vector of states
y	= sideforce coefficient
α, β, ϕ	= angle of attack, sideslip, and roll, respectively
δ	= oscillator damping parameter
ϵ	= coupling parameter
μ	= perturbed angle of attack
ρ	= air density
τ	= oscillator variable
ω	= oscillator frequency

Subscripts

$p, r, \ldots$	= stability derivatives with respect to $p, r, \ldots$
1, 3	= linear and cubic stability derivatives, respectively, with respect to β (when used with y, l, n)

Introduction

PERIODIC motions (or limit cycles) in lateral dynamics have been commonly observed on a variety of aircraft of diverse configuration. These limit cycle oscillations, primarily in roll and yaw, at moderate to high angles of attack have collectively been labeled as wing rock. Wing rock is undesirable because the oscillatory motion has adverse effects on maneuverability and reduces tracking accuracy. Also, simulations by Planeaux and Barth[1] show that an aircraft in wing rock may end up in a spin for certain control inputs.

This paper distinguishes between two types of wing rock. The first is called normal wing rock where the limit cycle oscillations build up gradually in amplitude with increasing angle of attack. This provides adequate warning to the pilot and, therefore, poses little threat to operational safety. Normal wing rock has been widely studied and modeled in the literature as will be described in the next section. In contrast, certain aircraft exhibit a rapid and discontinuous increase in limit cycle amplitude after onset of wing rock. This phenomenon is called large-amplitude wing rock. This is a more serious problem and needs to be avoided at all costs. Large-amplitude wing rock has been noticed in a recent bifurcation analysis of a model fighter aircraft reported by Planeaux et al.[2] The aim of this paper is to develop a minimal-order mathematical model for the aircraft dynamics that will characterize both normal and large-amplitude wing rock.

Some of the earliest studies of wing rock were carried out by Ross[3,4] using an aircraft lateral dynamic model with angle of attack as a parameter. This was consistent with observations of normal wing rock being a roll–yaw oscillation with near-constant angle of attack. Wing rock onset was shown[3] to be the result of a Hopf bifurcation as the Dutch roll mode goes unstable with increasing angle of attack. The amplitude and frequency of wing rock limit cycles have been calculated using various analytical techniques.[3,5,6] For the special case of aircraft with predominantly roll motion in wing rock, Liebst and Nolan[7] have recently used a simplified lateral dynamic model to predict wing rock onset.

At moderate to high angles of attack, the aerodynamic forces responsible for wing rock are nonlinear functions of the angle of attack. Wing rock of slender delta wings has, therefore, been studied[8] in an attempt to understand the fluid mechanics of the phenomenon and to help build a more general mathematical model for aircraft wing rock. Investigations into the mechanism of generation of wing rock in the case of slender delta wings have been reported[9,10] in recent years. Analytical models have been developed[11,12] to explain slender delta wing rock dynamics.

The methods of bifurcation theory have been employed by many researchers[13–15] to study nonlinear aircraft dynamics at high angles of attack. An eight-degree-of-freedom model is used[1] with the nonlinear aerodynamic functions obtained by curve fits from a database. Normal wing rock has been characterized by an onset at a Hopf bifurcation point followed by limit cycles gradually growing in amplitude with varying parameter values. Large-amplitude wing rock has been observed by Planeaux et al.[2] when a Hopf bifurcation signaling wing rock onset is followed by a pair of saddle-node bifurcations of the periodic branch. This results in a jump phenomenon at the saddle-node point leading to large-amplitude periodic motion.

The present study constructs a model that will display jump behavior of periodic solutions and that can be used to characterize wing rock limit cycles for an aircraft. Based on this model, it will be possible to pinpoint the causes leading to large-amplitude wing rock and to suggest ways of preventing this phenomenon.

Received April 20, 1995; revision received Nov. 20, 1995; accepted for publication Nov. 22, 1995.

*Visiting Faculty Member (Lecturer), Department of Aerospace Engineering.

†Professor, Department of Aerospace Engineering. Member AIAA.

Basic Model for Normal Wing Rock

The dynamic model for normal wing rock used by Ross[3] is adopted as the basic model for this study. The aircraft is assumed to be flying at a trim angle of attack. Longitudinal motion is considered negligible and the lateral-directional equations with angle of attack as a parameter are written in the stability axis system as

$$\dot{x} = f(x, \alpha) = F(\alpha)x + g(x, \alpha) \tag{1}$$

where $x = (\beta\ \phi\ p\ r)'$. Elements of the Jacobian matrix F and the vector of nonlinear terms g are given in Table 1. The aerodynamic derivatives are given as polynomial functions of the angle of attack α (as measured from its zero-lift value). The aircraft moments of inertia are appropriately calculated corresponding to each trim α. Data for the present study, adapted from Ross[3] and Cochran and Ho,[16] are given in Table 2. The data available are valid only for $\alpha < 20$ deg. Also nonlinear β derivatives are provided in Ref. 3 only for $\alpha = 14.3$ deg. Therefore, the present study assumes these nonlinear β derivatives to be constant with α.

The angle of attack for which the complex Dutch Roll eigenvalue pair of the Jacobian matrix F has zero real part signifies the Hopf bifurcation at the onset of wing rock. The root locus plot of the Dutch roll poles with α as the parameter is shown in Fig. 1. With increasing α, the complex eigenvalue pair is seen to cross the imaginary axis for $\alpha \approx 14$ deg. Wing rock limit cycles can be seen by numerically integrating Eq. (1) for an angle of attack greater than 14 deg. For example, using the data given in Table 2 for $\alpha = 14.3$ deg, the amplitude of limit cycle oscillations works out to nearly 5 deg in sideslip and about 35 deg in roll with a period of 2.6 s (Ref. 6).

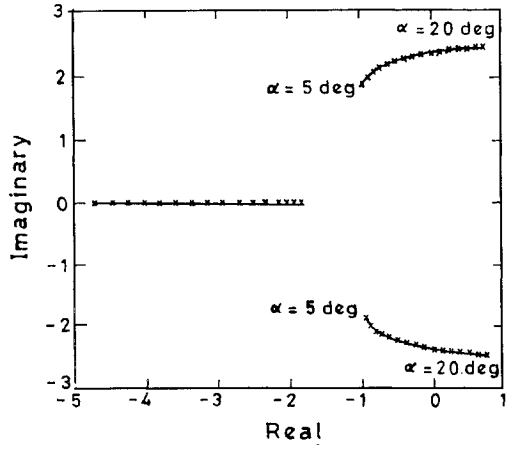

Fig. 1 Root locus of Dutch roll poles with parameter α.

Tracking Periodic Orbits

Numerical integration of the system equation (1), for a given α, until a stable periodic orbit is reached, does not by itself offer a solution to the problem of continuing the periodic orbit with varying parameter. Numerical integration in conjunction with a continuation algorithm, however, can be effectively used to track periodic solutions. A continuation algorithm for this purpose based on a shooting method for solving the nonlinear boundary value problem with mixed boundary conditions has been suggested by Holodniok and Kubicek.[17]

Shooting methods involve assuming an initial set of values for $x(0)$ and the time period T and numerically integrating the system equation (1) for one time period. The values of $x(T)$ so obtained are used to set up the functions

$$f(x, T; \alpha) = x(T) - x(0) \tag{2}$$

The initial guess for $x(0)$ and T is updated after every integration, whereas the functions in Eq. (2) are driven to zero by a continuation algorithm. This procedure converges to give the periodic solution $x(0) = x(T)$ and T for a particular α. Using this solution as a starting point, the continuation algorithm can track the periodic orbit with varying values of the parameter α.

The solution procedure requires $(n + 1)$ unknowns, n variables and T, to be calculated for a value of the parameter, but Eq. (2) provides only n conditions. The problem has been overcome by Holodniok and Kubicek[17] by arbitrarily fixing one component of the solution that is updated at regular intervals. Instead, the $(n + 1)$th condition can be obtained by observing[18] that the first-order ordinary differential equations representing a dynamical system usually arise from a set of second-order ordinary differential equations. That is, the variables occur in pairs representing a displacement and its associated velocity. Since the displacement variable satisfies $x(T) - x(0) = 0$, its velocity variable will take on the value zero somewhere in the interval $[0, T]$, say, t^*. This means that an extra condition can be imposed as $x_k(0) = 0$ for some appropriate choice of k. This merely amounts to shifting the time axis to t^*, a procedure that leaves the solutions of an autonomous system unaffected. Further details of the solution procedure are given in Ref. 19.

The Pittsburgh continuation (PITCON) algorithm of Rheinboldt[20] has been employed for the present study to track wing rock limit

Table 1 Elements of the F matrix and the g vector

$$F = \begin{bmatrix} 2k_1y_1 & (g/V)\cos\alpha & 2k_2y_p & -1 + 2k_2y_r \\ 0 & 0 & 1 & 0 \\ (k_3/i_x)(l_1 + i_2n_1) & 0 & (k_4/i_x)(l_p + i_2n_p) & (k_4/i_x)(l_r + i_2n_r) \\ (k_3/i_z)(n_1 + i_1l_1) & 0 & (k_4/i_z)(n_p + i_1l_p) & (k_4/i_z)(n_r + i_1l_r) \end{bmatrix}$$

$$g = \begin{pmatrix} 0.5bk_1y_3\beta^3 \\ 0 \\ (k_3/i_x)(l_3 + i_2n_3)\beta^3 \\ (k_3/i_z)(n_3 + i_1l_3)\beta^3 \end{pmatrix}$$

$k_1 = \rho SV/m$ $\quad k_2 = k_1(b/2V)$ $\quad k_3 = qSb/e$ $\quad k_4 = k_3(b/2V)$

$i_1 = i_{xz}/i_x$ $\quad i_2 = i_{xz}/i_z$ $\quad e = 1 - i_1i_2$ $\quad q = 0.5\,\rho V^2$

Table 2 Configuration, inertia, and aerodynamic data

$m = 2154$ kg	$b = 6.10$ m	$S = 40.18$ m^2
$V = 71.25$ m/s	$\rho = 1.2256$ kg/m^3	$g = 9.81$ m/s^2
$y_1 = -0.382$	$l_1 = 0.0371 - 0.7367\alpha$	$n_1 = 0.0657 + 0.3274\alpha$
$y_p = 0.014 + 0.505\alpha - 0.47\alpha^2$	$l_p = -0.132 + 0.08\alpha$	$n_p = 0.0125\alpha - 0.938\alpha^2$
$y_r = 0$	$l_r = 0.006 + 0.54\alpha$	$n_r = -0.351 - 0.089\alpha$
At $\alpha = 14.3$ deg		
$y_3 = -1.958$	$l_3 = 0$	$n_3 = 2.492$
$i_x = 2182$ kgm^2	$i_z = 25430$ kgm^2	$i_{xz} = 1615$ kgm^2

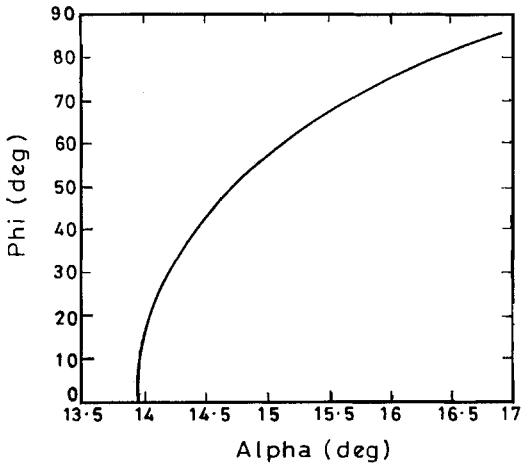

Fig. 2 Wing rock of basic model showing peak roll amplitude.

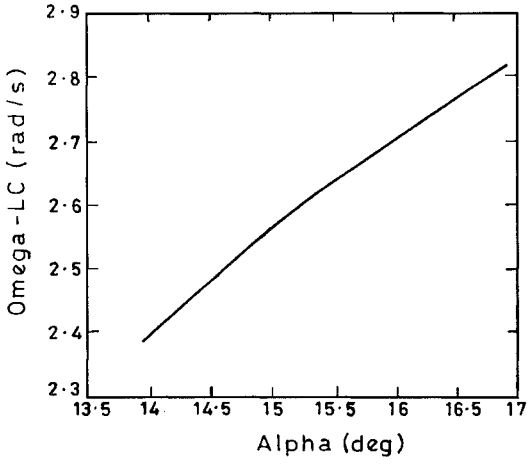

Fig. 3 Wing rock of basic model showing limit cycle frequency.

cycle orbits for Eq. (1). Roll angle being one of the variables, an extra condition is added to the set Eq. (2) by specifying the roll rate to be zero. This means that the point on the limit cycle at which roll rate is zero is used as the reference point for reckoning time. Starting values for the shooting method are available from a numerical integration at $\alpha = 14.3$ deg. Results obtained from the continuation run are plotted in Fig. 2 showing peak amplitude of roll angle, which is seen to increase gradually with increasing values of α. Figure 3 shows the increase in limit cycle frequency with increasing values of the parameter α. The wing rock in this case can be seen to be normal.

Large-Amplitude Wing Rock

The basic model for normal wing rock needs to be augmented for it to be capable of displaying a saddle-node bifurcation of its periodic branch. The variation with α of the aerodynamic derivatives in Eq. (1) is responsible for the Hopf bifurcation, whereas the cubic nonlinearities in β restrict the growth of the unstable mode, resulting in a limit cycle. Altering the α dependence of the aerodynamic derivatives will shift the Hopf bifurcation at wing rock onset to a different angle of attack, whereas further nonlinear terms in the lateral-directional variables will affect the amplitude and/or frequency of the limit cycles. Neither modification, however, is expected to bring about the required saddle-node bifurcation.

The study of Planeaux et al.[2] reveals that limit cycle oscillation of the lateral-directional variables in large-amplitude wing rock is accompanied by small limit cycle oscillations in angle of attack at twice the limit cycle frequency. This suggests a coupling between the lateral-directional and the longitudinal modes. We, therefore, consider the possibility of resonant interaction of a limit cycling system such as Eq. (1) with an external source resulting in multiple limit cycles and a jump at a periodic saddle-node bifurcation. Resonant excitation can be caused by either an external or a parametric forcing.[21,22] An external forcing, however, does not appear promising for the present problem. This leads us to investigate the possibility of a parametric interaction[23,24] with another mode.

One solution to this problem is to consider a parametric excitation to the system equation (1) from a hypothetical second-order harmonic oscillator, which in turn is forced by Eq. (1). This arrangement results in the limit cycling system and the harmonic oscillator being coupled to each other. We also require that the frequency of the harmonic oscillator be nearly twice that of the limit cycle:

$$\omega \approx 2\omega_{LC} \tag{3}$$

This is to ensure that the harmonic oscillator is resonantly excited.

Augmented Model

The augmented model is constructed as follows. The four first-order equations of Eq. (1) can be represented as

$$\dot{x}_i = f_i(x, \alpha), \qquad i = 1, \ldots, 4 \tag{4}$$

whereas the second-order oscillator can be written as

$$\ddot{\tau} + \delta\dot{\tau} + \omega^2\tau = 0 \tag{5}$$

Now, the oscillator in Eq. (5) is forced by a term $\epsilon x_i x_j$, where x_i and x_j are any two of the variables from Eq. (4) and ϵ is the coupling parameter. Since this forcing term acts at twice the limit cycle frequency, the harmonic oscillator is resonantly excited because of the condition given by Eq. (3).

The second-order system equation (5) with the forcing term added can be written as two first-order equations

$$\dot{\tau}_1 = \tau_2 \tag{6}$$

$$\dot{\tau}_2 = -\delta\tau_2 - \omega^2\tau_1 - \epsilon x_i x_j \tag{7}$$

The system [Eqs. (6) and (7)] is used to parametrically excite Eq. (4) as follows: We arbitrarily choose the first of the four equations (4) and add to it a forcing term $\tau_1 x_j$ (choosing the coefficient to be 1.0 with no loss of generality):

$$\dot{x}_1 = f_1(x, \alpha) + \tau_1 x_j \tag{8}$$

$$\dot{x}_i = f_i(x, \alpha), \qquad i = 2, \ldots, 4 \tag{9}$$

The frequency associated with τ_1 is approximately twice the limit cycle frequency. Thus, the limit cycling system equation (4) is being parametrically excited at nearly twice its natural frequency. Note that we may equally well have chosen any one or more of the four equations in Eq. (4) to add a parametric excitation term.

Specifically, the following values are chosen for the various parameters in the preceding equations: $\epsilon = 1.0$, $\delta = 0.2$, and $\omega = 4.8$. The harmonic oscillator is excited by the term $x_1 x_3$, which is the same as βp. The parametric forcing to the first of Eq. (4) is given by $\tau_1 x_3$, which is $\tau_1 p$ applied to the equation in β. Equations (6–9) constitute a set of six equations that represents our augmented model.

Computational Results

The shooting method is again employed to track the periodic solutions of this augmented system of six equations. The starting point for the continuation algorithm is provided by a numerical integration of the augmented equations for $\alpha = 14.3$ deg. Periodic solutions are then tracked with decreasing values of α as shown in Fig. 4, where peak values of the roll angle ϕ are plotted against the parameter α. Starting with the solution for $\alpha = 14.3$ deg in Fig. 4, continuing in the initial direction of decreasing α shows smaller roll angle solutions passing through two saddle-node bifurcation points. The value of α at the Hopf bifurcation indicating the point of wing rock onset can be seen to be identical to that for the basic model for normal wing rock in Fig. 2.

To capture the variation of peak values of oscillator variable τ_1 with α, the condition setting the roll rate to zero in the continuation procedure is replaced by $\tau_2 = 0$. The algorithm then tracks the

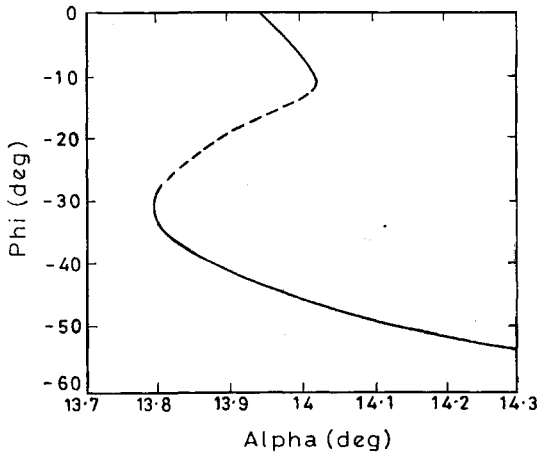

Fig. 4 Wing rock of augmented model showing peak roll amplitude: ——, stable and – – –, unstable.

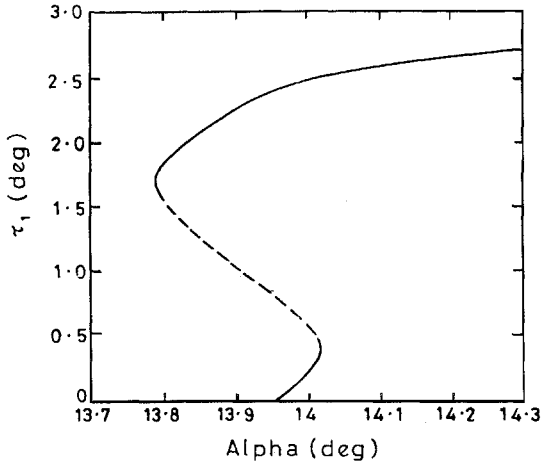

Fig. 5 Wing rock of augmented model showing peak oscillator variable amplitude: ——, stable and – – –, unstable.

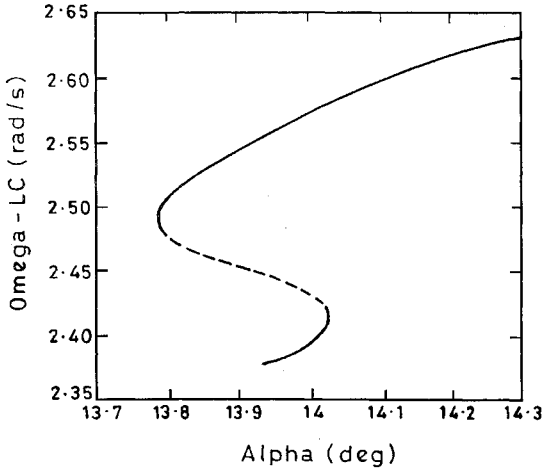

Fig. 6 Wing rock of augmented model showing limit cycle frequency: ——, stable and – – –, unstable.

periodic orbits with decreasing α, as displayed in Fig. 5. This is the same limit cycle solution as shown in Fig. 4 but plotted for a different variable. Figure 6 shows the variation of limit cycle frequency with α. Note that the first saddle-node bifurcation with increasing α occurs when the limit cycle frequency is close to half the oscillator frequency ($\omega = 4.8$). State–space projections of limit cycle trajectories are shown in Figs. 7 and 8. The p–β plot shows a single orbit, whereas the p–τ_1 plot shows two orbits indicating that the periodic oscillations in τ_1 are at twice the frequency of the limit cycle motion of the lateral variables.

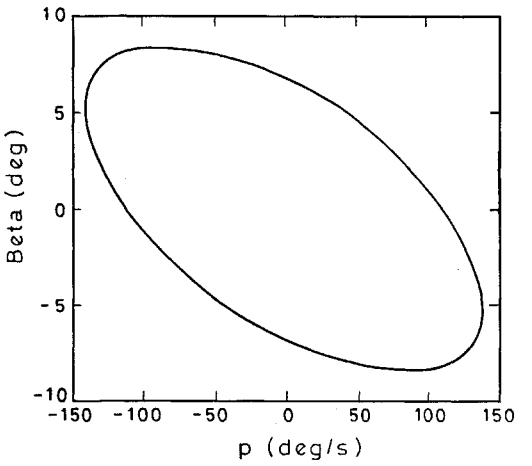

Fig. 7 Augmented model limit cycle orbit in p–β space.

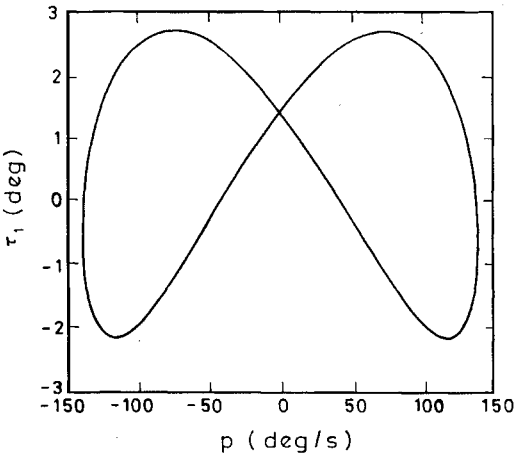

Fig. 8 Augmented model limit cycle orbit in p–τ_1 space.

Causes of Large-Amplitude Wing Rock

The preceding section has employed a hypothetical oscillator to build a model capable of displaying the bifurcation behavior representative of large-amplitude wing rock. It remains to identify the aircraft dynamic equations that can serve to augment the lateral-directional model Eq. (1), as outlined earlier.

In constructing the original model equation (1), it was assumed that for any α the longitudinal modes were negligible. If this assumption were relaxed allowing small perturbations about the longitudinal trim, these perturbation terms would enter the aircraft equations of motion as follows. (However, the aerodynamic coefficients are evaluated at the mean trim value of angle of attack.) Neglecting aerodynamic force terms along the Z axis for simplicity, and denoting the perturbed angle of attack about the stability axis as μ,

$$\dot{\mu} = q - p\beta \tag{10}$$

where the $p\beta$ term represents the kinematic coupling effect. Also,

$$\dot{q} = m_\mu \mu + m_q q + m_{\dot{\mu}} \dot{\mu} + m_{p\beta} p\beta + pr(i_z - i_x)/i_y \tag{11}$$

from which one can easily derive

$$\ddot{\mu} = m_\mu \mu + m_q q + m_{\dot{\mu}} \dot{\mu}$$

$$+ m_{p\beta} p\beta + pr(i_z - i_x)/i_y - p\dot{\beta} - \dot{p}\beta \tag{12}$$

Setting $\tau_1 = \mu$ and $\tau_2 = \dot{\mu}$, we get a second-order harmonic oscillator representing the short-period mode with forcing terms coming from the effect of kinematic coupling, inertia coupling, and the Magnus moment coefficient $m_{p\beta}$. This equation for the perturbed angle of attack μ plays the role of the harmonic oscillator parametrically exciting the aircraft lateral dynamics through the coupling term μp.

The preceding analysis reveals that large-amplitude wing rock is the result of lateral–longitudinal interaction caused primarily by

inertial and kinematic coupling. According to the formulation of the augmented model, large-amplitude wing rock occurs when the short-period frequency is nearly twice the Dutch roll (limit cycle) frequency. The onset of large-amplitude wing rock is identical to that of normal wing rock. The coupling terms, however, under the resonance condition equation (3), are responsible for a jump in the limit cycle amplitude characteristic of large-amplitude wing rock.

Prevention Strategies

The construction of the augmentation scheme naturally suggests ways of avoiding large-amplitude wing rock. One way is to control the coupling parameter ϵ, which is a measure of the interaction between the lateral and longitudinal modes. However, the nature of the coupling terms represented by ϵ makes it difficult to manipulate them as a means of avoiding large-amplitude wing rock.

A more effective strategy would be to detune the oscillator (short-period) frequency from a value near twice the limit cycle (Dutch roll) frequency. It is expected that by detuning the oscillator frequency from resonance, the periodic saddle-node point can be avoided. That this is indeed the case is illustrated in Fig. 9, where limit cycle amplitudes in roll are shown for three different frequencies ω of the harmonic oscillator keeping the values of $\delta = 0.2$ and $\epsilon = 1.0$ fixed. On decreasing ω, one turning point appears to vanish by coalescing with the Hopf bifurcation point, yielding a subcritical structure for $\omega = 4.5$. Then the other turning point also coalesces with the Hopf point, and for $\omega = 4.2$ in Fig. 9, the turning points and the unstable limit cycles have disappeared and the large-amplitude wing rock has been reduced to a normal one.

Solutions for the frequency of the limit cycle oscillation in the lateral variables are shown in Fig. 10 for the same set of values of ω. Twice ω_{LC} is plotted on the ordinate for easy verification of the resonance condition given by Eq. (3). These studies suggest that for a sufficiently large detuning the periodic saddle-node bifurcation can be avoided, thus preventing jump and reducing large-amplitude wing rock to normal wing rock. As a matter of further curiosity, the periodic saddle-node point does not seem to vanish[19] for a small increase (5%) in ω from the nominal value of 4.8. However, a more precise judgment of this point is not possible without nonlinear β data for α values beyond 14.3.

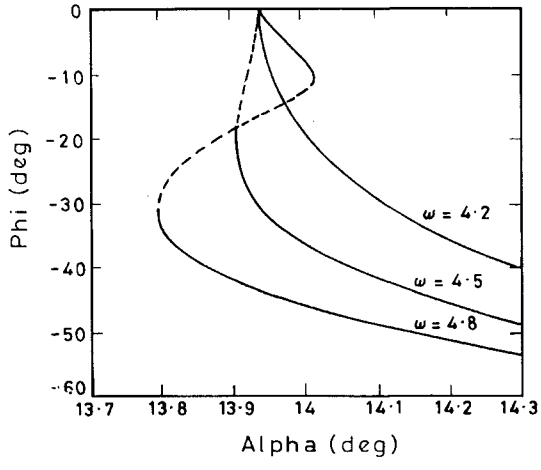

Fig. 9 Wing rock of augmented model showing peak roll amplitude for ω = 4.2, 4.5, and 4.8: ——, stable and – – –, unstable.

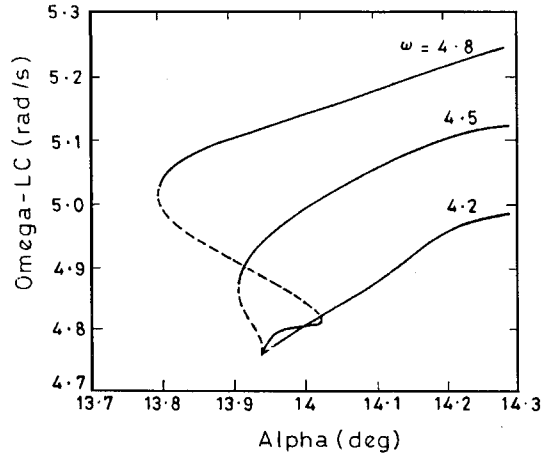

Fig. 10 Wing rock of augmented model showing limit cycle frequency for ω = 4.2, 4.5, and 4.8: ——, stable and – – –, unstable.

Conclusion

The present paper has studied periodic motions in aircraft lateral dynamics called wing rock. Two types of wing rock, normal and large amplitude, have been distinguished. A sixth-order dynamic model has been constructed that serves to characterize wing rock dynamics of both types. Wing rock onset occurs at a Hopf bifurcation of the lateral dynamic variables with parameter α. With increasing α, normal wing rock limit cycles build up gradually in amplitude, whereas large-amplitude wing rock results from a jump at a saddle-node bifurcation point of the periodic solutions.

The construction of the augmented model reveals one mechanism for large-amplitude wing rock. That is, large-amplitude wing rock is the result of lateral–longitudinal coupling by which the Dutch roll mode is parametrically excited by the short-period mode, whereas the short-period mode is forced near its natural frequency by the lateral variables. Inertial and kinematic coupling terms are primarily responsible for the jump in limit cycle amplitude, whereas the aerodynamic nonlinearities cause the onset of wing rock and restrict the unstable Dutch roll mode to a limit cycle.

Detuning the short-period frequency from the Dutch roll is indicated as a possible strategy to avoid large-amplitude wing rock. Although it is not possible to rule out a role for resonances of other orders in creating large-amplitude wing rock, there is no observation in the literature of their presence.

Acknowledgments

The authors would like to acknowledge the useful comments and information provided by one of the reviewers.

References

[1]Planeaux, J. B., and Barth, T. J., "High-Angle-of-Attack Dynamic Behavior of a Model High-Performance Fighter Aircraft," AIAA Paper 88-4368, 1988.

[2]Planeaux, J. B., Beck, J. A., and Baumann, D. D., "Bifurcation Analysis of a Model Fighter Aircraft with Control Augmentation," AIAA Paper 90-2836, 1990.

[3]Ross, A. J., "Investigation of Nonlinear Motion Experienced on a Slender-Wing Research Aircraft," *Journal of Aircraft*, Vol. 9, No. 9, 1972, pp. 625–631.

[4]Ross, A. J., "Lateral Stability at High Angles of Attack, Particularly Wing Rock," Paper 10, AGARD CP 260, Sept. 1978.

[5]Padfield, G. D., "Nonlinear Oscillations at High Incidence," AGARD CP 235, Paper 31, May 1978.

[6]Ananthkrishnan, N., and Sudhakar, K., "Prediction of Aircraft Wing Rock Using Describing Function Analysis," *Journal of the Aeronautical Society of India*, Vol. 46, No. 1, 1994, pp. 25–29.

[7]Liebst, B. S., and Nolan, R. C., "Method for the Prediction of the Onset of Wing Rock," *Journal of Aircraft*, Vol. 31, No. 6, 1994, pp. 1419–1421.

[8]Hsu, C.-H., and Lan, C. E., "Theory of Wing Rock," *Journal of Aircraft*, Vol. 22, No. 10, 1985, pp. 920–924.

[9]Ericsson, L. E., "Slender Wing Rock Revisited," *Journal of Aircraft*, Vol. 30, No. 3, 1993, pp. 352–356.

[10]Ericsson, L. E., and Hanff, E. S., "Further Analysis of High-Rate Rolling Experiments of a 65-Deg Delta Wing," *Journal of Aircraft*, Vol. 31, No. 6, 1994, pp. 1350–1357.

[11]Elzebda, J. M., Nayfeh, A. H., and Mook, D. T., "Development of an Analytical Model of Wing Rock for Slender Delta Wings," *Journal of Aircraft*, Vol. 26, No. 8, 1989, pp. 737–743.

[12]Nayfeh, A. H., Elzebda, J. M., and Mook, D. T., "Analytical Study of the Subsonic Wing-Rock Phenomenon for Slender Delta Wings," *Journal of Aircraft*, Vol. 26, No. 9, 1989, pp. 805–809.

[13]Carroll, J. V., and Mehra, R. K., "Bifurcation Analysis of Nonlinear Aircraft Dynamics," *Journal of Guidance, Control, and Dynamics*, Vol. 5, No. 5, 1982, pp. 529–536.

[14]Zagaynov, G. I., and Goman, M. G., "Bifurcation Analysis of Critical Aircraft Flight Regimes," International Council of the Aeronautical Sciences, ICAS-84-4.2.1, Sept. 1994, pp. 217–223.

[15]Jahnke, C., and Culick, F. E. C., "Application of Bifurcation Theory to the High-Angle-of-Attack Dynamics of the F-14," *Journal of Aircraft*, Vol. 31, No. 1, 1994, pp. 26–34.

[16]Cochran, J. E., and Ho, C.-S., "Stability of Aircraft Motion in Critical Cases," *Journal of Guidance, Control, and Dynamics*, Vol. 6, No. 4, 1983, pp. 272–279.

[17]Holodniok, M., and Kubicek, M., "DERPER—An Algorithm for the Continuation of Periodic Solutions in Ordinary Differential Equations," *Journal of Computational Physics*, Vol. 55, Aug. 1984, pp. 254–267.

[18]Reithmeier, E., *Periodic Solutions of Nonlinear Dynamical Systems*, Springer–Verlag, Berlin, 1991.

[19]Ananthkrishnan, N., "Continuation and Bifurcation Methods Applied to Nonlinear Problems in Flight Dynamics," Ph.D. Thesis, Aerospace Engineering Dept., Indian Inst. of Technology, Bombay, India, Feb. 1994.

[20]Rheinboldt, W. C., *Numerical Analysis of Parametrized Nonlinear Equations*, Wiley, New York, 1986.

[21]Schmidt, G., and Tondl, A., *Nonlinear Vibrations*, Cambridge Univ. Press, Cambridge, England, UK, 1986.

[22]Nayfeh, A. H., and Mook, D. T., *Nonlinear Oscillations*, Wiley, New York, 1979.

[23]Minorsky, N., *Nonlinear Oscillations*, Van Nostrand, New York, 1962.

[24]Cartmell, M., *Introduction to Linear, Parametric and Nonlinear Vibrations*, Chapman and Hall, London, 1990.